HIV disrupts CD34^{+} progenitors involved in T-cell differentiation

*Tetsuo Tsukamoto [1, 2, 3]

[1] The Kirby Institute for infection and immunity in society, University of New South Wales, Sydney, Australia

[2] Center for AIDS Research, Kumamoto University, Kumamoto, Japan

[3] Department of Immunology, Kindai University Faculty of Medicine, Osaka, Japan

*Corresponding author mailing address: Department of Immunology, Kindai University Faculty of Medicine, 377-2 Onohigashi, Osakasayama-shi, 589-8511 Osaka, Japan

Telephone: +81 72 366 0221

Fax: +81 72 367 7660

Email: ttsukamoto@med.kindai.ac.jp

Abstract

HIV-1 causes the loss of $CD4^+$ T cells via depletion or impairment of their production. The latter involves infection of thymocytes, but the involvement of other cells including haematopoietic $CD34^+$ cells remains unclear even though HIV-positive patients frequently manifest myelosuppression. This study utilised the OP9-DL1 coculture system, which supports in vitro T-lineage differentiation of human haematopoietic stem/progenitor cells. Cord-derived $CD34^+$ cells were infected with CXCR4-tropic HIV-1_{NL4-3} and cocultured. HIV-infected cocultures exhibited sustained viral replication for 5 weeks, as well as reduced $CD4^+$ T-cell growth at weeks 3–5. It was further revealed that $CD34^+CD7^+CXCR4^+$ cells can be quickly depleted as early as in 1 week after infection of the subset, and this was accompanied by the emergence of $CD34^+CD7^+CD4^+$ cells. These results indicate that CXCR4-tropic HIV-1 strains may disrupt $CD34^+CD7^+$ lymphoid progenitor cell pools, presumably leading to impaired T-cell production potential.

Keywords

human immunodeficiency virus, acquired immunodeficiency syndrome, haematopoietic stem/progenitor cells, C-X-C chemokine receptor type 4

37 **Introduction**

38

39 Human immunodeficiency virus (HIV) infection is associated with
40 haematological changes [1]. Antiretroviral therapy is effective in controlling viremia
41 and treating acquired immunodeficiency syndrome (AIDS). However, some patients
42 do not experience sufficient T-cell immune restoration despite being aviremic during
43 treatment [2]. HIV-infected patients may display decreased thymopoiesis [3]. Thymic
44 dysfunction occurs during HIV infection, and it is associated with rapid progression in
45 infants with prenatal HIV infection [4]. A previous report tested coculture of $CD34^+$ and
46 fetal thymic epithelial cells in the presence or absence of HIV-1, observing that
47 infection led to the inhibition of thymocyte maturation at early stages
48 ($CD44^+CD25^-CD3^-$) [5]. Pancytopenia may occur as a result of bone marrow
49 abnormalities in HIV-infected individuals [6,7]. A previous study revealed depletion of
50 $CD34^+CD4^+$ cells in bone marrow from HIV-infected patients. However, the study
51 failed to uncover evidence of HIV infection of these cells [8].

52 The thymopoiesis environment can be mimicked in vitro using the OP9-DL1 or
53 OP9-DL4 cell line. These cell lines were derived from the OP9 mouse stromal cell
54 line via transduction with a notch ligand called delta-like 1 (DL1) or DL4 [9,10]. The
55 ability of OP9-DL1 cells to support thymopoiesis in vitro was first demonstrated in
56 coculture with mouse cells [9]. The cell line is also known to support the differentiation
57 of human $CD34^+$ haematopoietic stem/progenitor cells (HSPCs) into thymocytes and
58 T cells [11]. There is evidence that OP9-DL1 cells produce stromal derived factor-1
59 (SDF-1, also known as CXCL12), a ligand for CXCR4 [12]. Although OP9-DL4 cells
60 can induce differentiation into both specific myeloid cells and T-lineage cells, OP9-
61 DL1 cells only permit the differentiation of T-lineage cells while inhibiting B cells

62 and myeloid cells [13]. Thus, the OP9-DL1 coculture system is used to investigate
63 events associated with T-lineage differentiation.

64 The chemokine receptors CXCR4 and CCR5 are common coreceptors for HIV-1
65 [14]. Control of CCR5-tropic strains of HIV-1 is usually considered a better correlate of
66 good clinical outcomes than control of CXCR4-tropic HIV-1 strains [15]. This is due to
67 the fact that memory $CD4^+$ T cells express higher levels of CCR5, thus making them
68 susceptible to CCR5-tropic HIV infection and subsequent depletion [16]. Consequently,
69 CCR5 may appear to be more closely involved in the immunopathogenesis of HIV
70 infection than CXCR4 [17]. Conversely, the biological functions of CXCR4 have been
71 well documented in fields such as developmental biology and haematology. CXCR4
72 interacts with SDF-1 and allows CXCR4-expressing cells to home to loci in which
73 SDF-1 is highly expressed [18]. SDF-1 and CXCR4 are essential in human stem cell
74 homing and repopulation of the host with differentiated haematopoietic cells [19,20].
75 SDF-1 is also produced by thymic epithelial cells, and it plays an important role in
76 migration of immature progenitors in the thymus [21].

77 Therefore, it may be important to better understand the influence of CXCR4-
78 tropic HIV-1 infection on CXCR4-associated biological events including
79 haematopoiesis and T-cell development [22]. A prior study sought to clarify the effect of
80 CXCR4-tropic simian-human immunodeficiency virus infection on T-lineage cell
81 production in the thymi of newborn rhesus macaques [23]. However, it is not realistic to
82 closely follow in vivo bone marrow/thymus events in HIV-infected individuals.
83 Instead, humanised mouse models can be beneficial for this purpose [24,25]. Moreover,
84 an easy-to-use ex-vivo model may be helpful for closely monitoring the
85 differentiation of HSPCs into T-lineage cells in the presence of HIV-1. The present

86 study aimed to determine the in vitro fate of $CD34^+$ progenitor cells and derivatives

87 exposed to HIV-1 using the OP9-DL1 coculture system.

88 **Results**

89

90 *Persistent HIV-1 infection observed in OP9-DL1 cocultures with cord-derived CD34$^+$*
91 *cells*

92 Two separate in vitro experiments were performed in the study. The data for
93 experiment 1 (long coculture) are shown in Figs. 1–3 and Extended Data Figs. 1–5.
94 To follow the in vitro fate of HIV–pre-exposed CD34$^+$ cells and derivatives for
95 several weeks, primary human umbilical cord-derived CD34$^+$ cells were infected with
96 HIV-1. These cells were partially CD4$^+$ and/or CXCR4$^+$ before infection (Extended
97 Data Fig. 1A). Cells were seeded in 48-well plates and exposed to 200 ng (p24) of
98 HIV-1$_{NL4-3}$. Following centrifugation and overnight incubation in the presence of
99 HIV-1, the cells were cocultured with OP9-DL1 cells (Fig. 1A). After a week of
100 coculture, intracellular HIV-1 p24 was detected in both CD34$^+$ and CD34$^-$ cells (Fig.
101 1B). HIV infection was further examined via magnetic bead separation of CD34$^+$ and
102 CD34$^-$ cells followed by DNA extraction and detection of HIV-1 *gag* DNA using
103 PCR (Extended Data Fig. 1B). The HIV-infected samples displayed persistent HIV-1
104 p24 expression in 0.1–1.7% of the total cocultured human cells (Fig. 1C, Extended
105 Data Fig. 1C–G). A correlation was found between intracellular HIV-1 p24$^+$ cell
106 counts and supernatant HIV-1 p24 concentrations (Extended Fig. 1E).

107

108 *The dynamics of CD4$^+$ cells in OP9-DL1 cocultures with HIV–pre-exposed CD34$^+$*
109 *cells*

110 The influence of HIV pre-exposure of CD34$^+$ cells on post-coculture events was
111 analysed by flow cytometry weekly until week 5. CD19$^+$, CD20$^+$ or CD33$^+$ cells were
112 not detected in the samples tested (data not shown). HIV-infected cocultures had

113 significantly lower whole cell counts at weeks 3, 4 and 5 post-coculture than
114 uninfected cocultures (Extended Data Fig. 2A), demonstrating reduced cell growth in
115 the presence of HIV-1. Similarly, the $CD4^+CD8^+$ and $CD4^+CD8^+CXCR4^+$ cell counts
116 were significantly smaller in HIV^+ cocultures than in HIV^- cocultures at week 3
117 (Extended Data Fig. 2B–D). When $CD34^-$ cells were gated and analysed for CD7 and
118 CD4 expression (Fig. 2A), the $CD34^-CD7^+CD4^+$ cell counts were not significantly
119 different between HIV-infected and uninfected samples (Fig. 2B). By contrast, there
120 was a notable decline in $CD34^-CD7^-CD4^+$ cell counts in HIV^+ samples compared to
121 those in HIV^- samples at week 3 (Fig. 2C). Further analysis of $CD34^-$ cells revealed
122 that the $CD7^+CD4^+$ cells contained CD4/CD8 double-positive cells and $CD3^+CD4^+$
123 cells, whereas the $CD7^-CD4^+$ cells were mostly $CD3^+CD4^+$ cells (Extended Data Fig.
124 3). In the analysis of $CD34^-CXCR4^+$, $CD34^-CD7^+CXCR4^+$ and $CD34^-CD7^-CXCR4^+$
125 cells, the $CD34^-CD7^-CXCR4^+$ cells exhibited the greatest growth impairment
126 following HIV-1 infection (Extended Data Fig. 4).
127
128 *The dynamics of $CD34^+$ cells in OP9-DL1 cocultures with HIV–pre-exposed $CD34^+$*
129 *cells*
130 HIV infection of $CD34^+$ cells was detected by intracellular $p24^+$ staining
131 followed by flow cytometric analysis (Fig. 3A–B, Extended Data Fig. 5A–D).
132 $p24^+CD34^+$ cells failed to grow by week 2 (Fig. 3A), in contrast to the rapid growth of
133 $p24^+$ cells at this time point (Fig. 1C). $p24^+CD34^+CD7^+$ cell counts increased at weeks
134 2 and 3 (Fig. 3B) in association with a low average $CD34^+CD7^+$ cell count in week 1
135 after infection and a rapid increase in week 2 (Fig. 3C). Then, $CD34^+$ cell dynamics in
136 HIV^+ samples were compared with those in HIV^- samples (Fig. 3C-D, Extended Data
137 Fig. 5E–G). There were nonsignificant differences in $CD34^+CD7^+$ cell counts

138 between HIV^+ and HIV^- cocultures (Fig. 3C). The difference in the average
139 frequencies of $CD34^+CD7^+$ cells was greatest at week 3 (Fig. 3C). However, the
140 average $CD34^+CD7^+CXCR4^+$ cell count in HIV^+ cocultures versus that in HIV^-
141 cocultures exhibited the greatest difference at week 2 (Fig. 3D). Therefore,
142 $CD34^+CD7^+CXCR4^+$ cells may be affected by HIV-1 earlier than the entire
143 $CD34^+CD7^+$ cell population or cells of other phenotypes.
144
145 *HIV-1$_{NL4-3}$ infection of HSPC-derived cells after 4–6 weeks of coculture with OP9-*
146 *DL1 cells*
147 To better describe the effect of HIV infection on the short-term dynamics of
148 $CD34^+$ cells, experiment 2 was performed (short coculture, n = 12, Fig. 4A). The
149 experiment 2 results are shown in Figs. 4–6, Extended Data Figs. 6–8 and Extended
150 Data Tables 1–2. Briefly, coculture of OP9-DL1 cells with HIV-uninfected cord-
151 derived $CD34^+$ cells for 4–6 weeks produced a mixture of cells with different
152 phenotypes as determined by the expression of CD34, CD4, CD8, CD7 and CXCR4
153 (Figs. 1–3, Extended Data Figs. 1–5). CD4 expression levels in $CD34^+$ cells before
154 infection were lower than those in $CD34^-$ cells (Fig. 4B). Cells were then harvested
155 and infected with HIV-1$_{NL4-3}$ following the procedures for HIV infection of $CD34^+$
156 cells (Fig. 1A). The infected cells were cocultured again with a new OP9-DL1
157 monolayer and further incubated for 1 week (Fig. 4A). One week after infection, HIV
158 replication was detected in all HIV-infected samples (Fig. 4C). The majority of HIV-1
159 $p24^+$ cells were $CD34^-$ (Fig. 4C, Extended Data Fig. 6). The majority of $p24^+CD34^+$
160 cells were $CD7^+$ (Fig. 4C, Extended Data Table 1).
161

162 *Partial loss of $CD34^+CD7^+CXCR4^+$ cells after HIV-1_{NL4-3} infection of OP9-DL1–*
163 *cocultured cells*

164 The phenotypes of the cells in experiment 2 (short coculture) were analysed 1
165 week after infection (Fig. 5, Extended Data Fig. 7, Extended Data Table 2). The
166 whole cell counts were obtained using parts of the tested batches, with no significant
167 differences noted between HIV^+ and HIV^- samples (n = 4, p = 0.5000, Extended Data
168 Table 2). The frequencies of $CD4^+CD8^+$, $CD34^+$ and $CD34^+CD7^+$ cells were not
169 significantly different between HIV^+ and HIV^- cocultures (Extended Data Fig. 7).
170 Regarding CXCR4 expression levels in different subsets, the frequencies of
171 $CD34^+CD7^+CXCR4^+$ cells in HIV^+ samples were significantly reduced compared to
172 those in HIV^- samples (Fig. 5A and C middle). This may be in accordance with the
173 results in Fig. 3D in which the growth of $CD34^+CD7^+CXCR4^+$ cells slowed earlier (at
174 week 2) than those of other phenotypes (at week 3).

175

176 *Increased number of $CD34^+CD7^+CD4^+$ cells after HIV-1_{NL4-3} infection of OP9-DL1–*
177 *cocultured cells*

178 Figure 5 indicates the distinct dynamics of $CD34^+CD7^+CXCR4^+$ cells in the
179 presence of HIV-1. For increased clarity, $CD34^+CD7^+$ cells were further analysed for
180 CD4 expression (Fig. 6, Extended Data Fig. 8). Surprisingly, HIV-infected samples
181 had higher frequencies of $CD34^+CD7^+CD4^+CXCR4^+$ cells than uninfected samples
182 (Fig. 6A and B). These cells were found to be partially HIV $p24^+$ after carefully
183 adjusting the compensation matrices of the flow cytometry data (Fig. 6A and C). One
184 of nine batches was selected for further analyses of $CD34^+CD7^+CD4^+$ cells. Both the
185 frequencies and CD4 fluorescence intensities of $CD34^+CD7^+CD4^+$ cells were higher
186 in HIV^+ samples than in HIV^- samples (Extended Fig. 8B), implying the emergence

187 of $CD34^{+}CD7^{+}CD4^{hi}$ cells. In addition, the frequencies of $CD34^{+}CD7^{+}CD4^{+}CXCR4^{+}$

188 cells were correlated with those of $p24^{+}$ cells (Fig. 6D). A separate staining of an

189 experiment 2 sample with annexin V at week 1 after infection didn't result in

190 increased annexin V reactivity of $CD34^{+}CD4^{+}$ cells in HIV^{+} samples compared to

191 those in HIV^{-} samples (data not shown).

192 **Discussion**

193

194 Regarding the dynamics of $CD34^+$ cells in HIV-infected individuals, there has
195 been a debate regarding whether HSPCs comprise an unignorable viral reservoir [26].
196 There is also a possibility of modified turnover of HSPCs through HIV infection and
197 depletion of $CD4^+$ cells. For example, HIV infection commonly manifests as bone
198 marrow abnormalities [7]. Some patients fail to exhibit $CD4^+$ T-cell recovery even after
199 effective antiretroviral therapy, thus being termed immunological nonresponders.
200 Such immunological nonresponsiveness can be associated with immune activation
201 and/or bone marrow impairment [27,28]. To approach these problems, the present study
202 revealed a method for utilising the OP9-DL1 coculture system, which enables in vitro
203 follow-up of the early events in T-cell differentiation such as lymphoid progenitor cell
204 generation that normally occur in the bone marrow as well as $CD4^+$ thymocyte
205 differentiation in the thymus. The events observed in the cocultures of OP9-DL1 and
206 human $CD34^+$ cells are likely to involve interactions between SDF-1 and CXCR4, as
207 mouse SDF-1 expressed by OP9-DL1 cells has high amino acid sequence identity
208 with human SDF-1 [29]. The observation is in accordance with previous reports
209 illustrating that the SDF-1/CXCR4 pair is crucially involved in the homing and
210 repopulation of HSPCs in specific bone marrow niches [30] and the entire T-cell
211 developmental process in the thymus [21,31]. It has been reported that HSPCs and
212 thymocytes express CXCR4, but their CCR5 expression is limited [32]. Another report
213 indicated that HIV utilises CXCR4 when it infects multipotent progenitor cells [33].
214 CXCR4-tropic HIV strains might contribute to pathogenesis by interfering with
215 haematopoiesis and/or lymphopoiesis [34-36], although the underlying mechanisms are
216 yet to be unveiled.

217 The present results provide insights into the impact of HIV-1 on T-lineage
218 differentiation of haematopoietic progenitor cells. To be more physiological than the
219 previous studies analysing the influence of HIV on $CD34^+$ cells, the present study
220 didn't include strong stimuli such as 50–100 ng/mL of stem cell factor,
221 thrombopoietin, FMS-like tyrosine kinase 3 ligand or interleukin 3 [33,37]. In experiment
222 1 (long coculture), HIV-infected samples exhibited similar $CD4^+$ cell production rates
223 as uninfected samples at weeks 1 and 2 but reduced $CD4^+$ cell production rates from
224 week 3 to week 5 (Fig. 2). This was most clearly observed with the dynamics of
225 $CD34^-CD7^-CD4^+$ cells (Fig. 2C) that were mostly $CD3^+$ T cells (Extended Data Fig.
226 3). It is unclear how the reduction of cell growth at week 3 after infection was so
227 accurately reproduced in the 12 samples tested (Fig. 2C, individual data not shown).
228 However, in the subsequent analyses of $CD34^+$ cells, the growth rates of
229 $CD34^+CD7^+CXCR4^+$ cells tended to fall as early as week 2 (Fig. 3D). This was
230 observed in 7/12 samples tested (data not shown), and the decline occurred earlier
231 than the reduction in $CD34^-CD7^-CD4^+$ cell counts (week 3). Because $CD34^+CD7^+$
232 cells represent lymphoid progenitor cells [38,39], their involvement in defining the
233 production rates of $CD4^+$ cells may be speculated.

234 Subsequently, experiment 2 (short coculture, Figs. 4–6) was conducted to
235 examine the effects of HIV-1 on the short-term dynamics of T-lineage cells including
236 $CD34^+$ progenitors. HIV-1 infection resulted in significant decreases of the frequency
237 of $CD34^+CD7^+CXCR4^+$ cells 1 week after infection (Fig. 5B right), which may be
238 consistent with the results of experiment 1 (Fig. 3D). Because of the limitation of the
239 present study, the fate of the lost $CD34^+CD7^+CXCR4^+$ cells in the HIV^+ cocultures is
240 unknown. The differentiation capacity of the remaining $CD34^+CD7^+CXCR4^+$ cells
241 also remains untested. Interestingly, a recent article reported that bone marrow $CD34^+$

242 progenitor cells from HIV-infected patients exhibit impaired T-cell differentiation
243 potential [40], which was related to proinflammatory cytokines. Cytokine analyses may
244 be applicable to the coculture assays established in the present study.

245 The $CD34^+CD7^+$ progenitors were further analysed to better understand their
246 association with HIV-1 infection. Interestingly, the frequencies of $CD34^+CD7^+CD4^+$
247 cells were elevated in HIV-infected samples compared to those in uninfected samples
248 (Fig. 6, Extended Data Fig. 8). In addition, $CD34^+CD7^+CD4^+$ cells were found to be
249 partially HIV $p24^+$ (Fig. 6A and C). It may be fascinating to interpret the results as
250 CD4 upregulation following HIV infection, thereby driving the differentiation of T-
251 lineage precursor cells. However, caution may be necessary because exclusion of
252 possible CD34 upregulation in the infected $CD4^+$ cells was not confirmed in this
253 study (Extended Data Fig. 8), although the flow cytometry data did not indicate
254 correlations between HIV p24 expression and CD34 upregulation in $CD34^{low}$ cells
255 (data not shown). Further studies may be designed to test shorter coculture periods
256 than 1 week and/or investigate the association of HIV-1 infection with factors that
257 regulate the expression of CD3, CD4, CD7 and CD34. Such analyses will also help
258 better clarify the debate on the issues of $CD34^+$ viral reservoirs [26].

259 The findings in this article highlight the potential of anti-HIV treatments such as
260 gene therapy using $CD34^+$ HSPCs followed by transplantation because in this manner,
261 all haematopoietic events in the host can be protected against HIV infection by the
262 gene products even in the absence of effective immune responses [41]. The problem is
263 that although CCR5 may be considered a reasonable target for knockout or
264 knockdown to prevent infection by CCR5-tropic HIV strains, CXCR4 expression
265 should not be altered in HSPCs because of the essential biological functions of the
266 molecule [42]. Therefore, instead of modulating CXCR4 expression, anti-HIV

267 modalities targeting an HIV gene or component may be desirable for protecting
268 haematopoietic cells including T-lineage cells from CXCR4-tropic HIV infection [43].
269 In summary, the results of the long/short coculture of human $CD34^+$ cells and
270 derivatives with OP9-DL1 cells in the presence of HIV-1 indicate that the dynamics
271 of $CD34^+CD7^+$ lymphoid progenitors may be affected more quickly by HIV-1 than
272 $CD34^-CD4^+$ thymocytes and T cells despite the lower susceptibility of $CD34^+CD7^+$
273 cells to HIV-1 infection as suggested by their lower CD4 expression levels. Further
274 studies may be designed to elucidate the underling mechanisms. In addition, the
275 preceding reduction of $CD34^+CD7^+CXCR4^+$ cell growth at week 2 followed by the
276 reduction of $CD34^-CD4^+$ cell growth at week 3 in the HIV^+ cocultures may illustrate
277 the mechanism by which reduced sizes of progenitor cell pools may decelerate the
278 production of T cells in HIV-infected patients (Extended Data Fig. 9). This may occur
279 in combination with different mechanisms of $CD4^+$ T-cell depletion including direct
280 cytopathic effects, apoptosis and antigen-specific immunological mechanisms [44-46].

281 **Methods**

282

283 **Virus stocks.** Stocks of HIV-1_{NL4-3} were produced via transfection of 293T cells with
284 the molecular clone DNA pNL4-3 [47]. After transfection, the culture supernatant was
285 collected, and viral loads were determined using an HIV p24 enzyme-linked
286 immunosorbent assay (ELISA) kit (ZeptoMetrix, NY, USA).

287

288 **Cells.** Umbilical cord blood samples were collected at Fukuda Hospital, Kumamoto,
289 Japan after obtaining informed consent. Cord blood mononuclear cells were isolated
290 using Pancoll (PAN-Biotech GmbH, Aidenbach, Germany) and centrifugation at 800
291 rpm for 20 min. $CD34^+$ cells were labelled and selected using human CD34
292 microbeads and LS columns (Miltenyi Biotec, NSW, Australia). The purity constantly
293 exceeded 92%. The OP9-DL1 cell line was generated via retroviral transduction of
294 the OP9 cell line (RCB1124, Riken, Tsukuba, Japan) with human DL1. The cell line
295 was maintained in α-MEM medium (Wako Pure Chemical Industries, Osaka, Japan)
296 supplemented with 10% heat inactivated fetal bovine serum (FBS, GE Healthcare,
297 Tokyo, Japan).

298

299 **Antibodies.** Anti-human CD8 Brilliant Violet (BV) 510 (clone RPA-T8), anti-human
300 CD3 PE-Cy7 (clone UCHT1) and anti-human CD34 APC (clone 8G12) were
301 purchased from BD Biosciences (NSW, Australia). Anti-human CD4 PE-Cy7 (clone
302 OKT4), anti-human CD4 PerCP-Cy5.5 (clone OKT4) and anti-human CXCR4
303 BV421 (clone 12G5) were purchased from BioLegend (CA, USA). Anti-human CD3
304 ECD (clone UCHT1) and anti-HIV-1 p24 PE (clone FH190-1-1, also known as KC57

305 RD1) were purchased from Beckman Coulter (NSW, Australia). Anti-human CD7
306 FITC (clone CD7-6B7) was purchased from CALTAG Laboratories (CA, USA).
307
308 **Coculture of human cells with OP9-DL1.** The OP9-DL1 coculture experiment was
309 performed following a previously published protocol with modifications [48]. Briefly, 2
310 × 10^5 HIV-infected or uninfected cord-derived $CD34^+$ cells were seeded in a 6-well
311 plate (Corning, VIC, Australia) containing a OP9-DL1 monolayer. The coculture was
312 maintained for 5 weeks in α-MEM medium supplemented with 20% heat inactivated
313 FBS, 5 ng/mL recombinant human FMS-like tyrosine kinase 3 ligand (R&D Systems,
314 MN, USA) and 5 ng/mL recombinant human interleukin 7 (Miltenyi Biotec). Cells
315 were passaged weekly with vigorous pipetting and filtering through a 70-µm
316 membrane and cocultured again with a fresh monolayer of OP9-DL1 cells. A portion
317 of the collected cells was analysed by flow cytometry.
318
319 **HIV infection.** The method for in vitro HIV infection of $CD34^+$ cells was described
320 previously [49]. To infect primary cord-derived $CD34^+$ cells with HIV-1_{NL4-3}, a 48-well
321 plate (Corning) was treated overnight with RetroNectin (Takara Bio, Kusatsu, Japan)
322 at a concentration of 10 µg/mL. $CD34^+$ cells were re-suspended in the OP9-DL1
323 medium, seeded at 2 × 10^5 per well in the coated plate and infected with 200 ng (p24)
324 of HIV-1_{NL4-3} using spinoculation at 1200 × *g* at 34°C for 30 min. Cells were further
325 cultured overnight and cocultured in a 6-well plate with a fresh monolayer of OP9-
326 DL1 cells. For HIV infection of OP9-cocultured human cells, the cell concentration
327 was modified to 5 × 10^5 per well.
328

329 **Flow cytometry.** Surface and intracellular antigen expression was analysed using a
330 FACS LSR II (BD Biosciences), FACS Diva v6.0 software (BD Biosciences) and
331 FlowJo v10.3 software (FlowJo, OR, USA). Dead cells were discriminated using
332 Live/Dead Fixable Near-IR Dead Cell Stains (Thermo Fisher Scientific, VIC,
333 Australia). Live cells were further gated to exclude doublets from the analysis by
334 plotting FSC-H and FSC-A.
335
336 **PCR analysis of HIV DNA.** Cellular DNA was extracted using a Kaneka Easy DNA
337 Extraction Kit (Kaneka, Takasago, Japan). DNA extraction was followed by the PCR
338 analysis using an HIV *gag* primer set (sense: 5′-
339 AGTGGGGGGACATCAAGCAGCCATGCAAAT-3′, antisense: 5′-
340 TACTAGTAGTTCCTGCTATGTCACTTCC-3′) as described previously [50]. The
341 oligo DNAs were purchased from Sigma-Aldrich (Tokyo, Japan).
342
343 **Statistical analysis.** Statistical analysis was performed using GraphPad Prism
344 software version 7.0 (GraphPad Software, CA, USA). Statistical significance was
345 defined as $P < 0.05$. Comparisons between HIV-infected and uninfected samples were
346 performed using Wilcoxon's matched-pairs signed rank test, unless otherwise stated.
347 Multiple comparison analyses were done, if necessary, using Dunn's method.
348 Spearman's correlation coefficients were calculated for correlation analyses.
349
350 **Data availability.** The data that support the findings of this study are available from
351 the corresponding author upon reasonable request.

352 **References**

353 1 Parinitha, S. & Kulkarni, M. Haematological changes in HIV infection with
354 correlation to CD4 cell count. *Australas Med J* **5**, 157-162,
355 doi:10.4066/AMJ.20121008 (2012).

356 2 Corbeau, P. & Reynes, J. Immune reconstitution under antiretroviral
357 therapy: the new challenge in HIV-1 infection. *Blood* **117**, 5582-5590,
358 doi:10.1182/blood-2010-12-322453 (2011).

359 3 Blom, M., Epeldegui, M. & Uittenbogaart, C. H. in *HIV-Host Interactions*
360 (ed Theresa Li-Yun Chang) (InTech, 2011).

361 4 Ye, P., Kirschner, D. E. & Kourtis, A. P. The thymus during HIV disease:
362 role in pathogenesis and in immune recovery. *Curr HIV Res* **2**, 177-183 (2004).

363 5 Knutsen, A. P., Roodman, S. T., Freeman, J. J., Mueller, K. R. & Bouhasin,
364 J. D. Inhibition of thymopoiesis of CD34+ cell maturation by HIV-1 in an in vitro
365 CD34+ cell and thymic epithelial organ culture model. *Stem Cells* **17**, 327-338,
366 doi:10.1002/stem.170327 (1999).

367 6 Alexaki, A. & Wigdahl, B. HIV-1 infection of bone marrow hematopoietic
368 progenitor cells and their role in trafficking and viral dissemination. *PLoS Pathog* **4**,
369 e1000215, doi:10.1371/journal.ppat.1000215 (2008).

370 7 Dhurve, S. A. & Dhurve, A. S. Bone Marrow Abnormalities in HIV Disease.
371 *Mediterr J Hematol Infect Dis* **5**, e2013033, doi:10.4084/MJHID.2013.033 (2013).

372 8 Banda, N. K. *et al.* Depletion of CD34+ CD4+ cells in bone marrow from
373 HIV-1-infected individuals. *Biol Blood Marrow Transplant* **5**, 162-172,
374 doi:10.1053/bbmt.1999.v5.pm10392962 (1999).

375 9 Nakano, T., Kodama, H. & Honjo, T. Generation of lymphohematopoietic
376 cells from embryonic stem cells in culture. *Science* **265**, 1098-1101 (1994).

377 10 Schmitt, T. M. *et al.* Induction of T cell development and establishment of
378 T cell competence from embryonic stem cells differentiated in vitro. *Nat Immunol* **5**,
379 410-417, doi:10.1038/ni1055 (2004).
380 11 De Smedt, M., Hoebeke, I. & Plum, J. Human bone marrow CD34+
381 progenitor cells mature to T cells on OP9-DL1 stromal cell line without thymus
382 microenvironment. *Blood Cells Mol Dis* **33**, 227-232,
383 doi:10.1016/j.bcmd.2004.08.007 (2004).
384 12 Janas, M. L. *et al.* Thymic development beyond beta-selection requires
385 phosphatidylinositol 3-kinase activation by CXCR4. *J Exp Med* **207**, 247-261,
386 doi:10.1084/jem.20091430 (2010).
387 13 Mohtashami, M. *et al.* Direct comparison of Dll1- and Dll4-mediated Notch
388 activation levels shows differential lymphomyeloid lineage commitment outcomes. *J*
389 *Immunol* **185**, 867-876, doi:10.4049/jimmunol.1000782 (2010).
390 14 Weiss, R. A. HIV receptors and the pathogenesis of AIDS. *Science* **272**,
391 1885-1886 (1996).
392 15 Grivel, J. C. & Margolis, L. B. CCR5- and CXCR4-tropic HIV-1 are
393 equally cytopathic for their T-cell targets in human lymphoid tissue. *Nat Med* **5**,
394 344-346, doi:10.1038/6565 (1999).
395 16 Schnittman, S. M. *et al.* Preferential infection of CD4+ memory T cells by
396 human immunodeficiency virus type 1: evidence for a role in the selective T-cell
397 functional defects observed in infected individuals. *Proc Natl Acad Sci U S A* **87**,
398 6058-6062 (1990).
399 17 Okoye, A. A. & Picker, L. J. CD4(+) T-cell depletion in HIV infection:
400 mechanisms of immunological failure. *Immunol Rev* **254**, 54-64,
401 doi:10.1111/imr.12066 (2013).

402 18 Kucia, M. *et al.* CXCR4-SDF-1 signalling, locomotion, chemotaxis and
403 adhesion. *J Mol Histol* **35**, 233-245 (2004).
404 19 Lapidot, T. & Kollet, O. The essential roles of the chemokine SDF-1 and its
405 receptor CXCR4 in human stem cell homing and repopulation of transplanted
406 immune-deficient NOD/SCID and NOD/SCID/B2m(null) mice. *Leukemia* **16**, 1992-
407 2003, doi:10.1038/sj.leu.2402684 (2002).
408 20 Kucia, M. *et al.* Trafficking of normal stem cells and metastasis of cancer
409 stem cells involve similar mechanisms: pivotal role of the SDF-1-CXCR4 axis. *Stem*
410 *Cells* **23**, 879-894, doi:10.1634/stemcells.2004-0342 (2005).
411 21 Plotkin, J., Prockop, S. E., Lepique, A. & Petrie, H. T. Critical role for
412 CXCR4 signaling in progenitor localization and T cell differentiation in the
413 postnatal thymus. *J Immunol* **171**, 4521-4527 (2003).
414 22 Berkowitz, R. D., Beckerman, K. P., Schall, T. J. & McCune, J. M. CXCR4
415 and CCR5 expression delineates targets for HIV-1 disruption of T cell
416 differentiation. *J Immunol* **161**, 3702-3710 (1998).
417 23 Suzuki, H. *et al.* Intrathymic effect of acute pathogenic SHIV infection on
418 T-lineage cells in newborn macaques. *Microbiol Immunol* **49**, 667-679,
419 doi:10.1111/j.1348-0421.2005.tb03646.x (2005).
420 24 Marsden, M. D. *et al.* HIV latency in the humanized BLT mouse. *J Virol* **86**,
421 339-347, doi:10.1128/jvi.06366-11 (2012).
422 25 Dudek, T. E. & Allen, T. M. HIV-specific CD8(+) T-cell immunity in
423 humanized bone marrow-liver-thymus mice. *J Infect Dis* **208 Suppl 2**, S150-154,
424 doi:10.1093/infdis/jit320 (2013).
425 26 Pace, M. & O'Doherty, U. Hematopoietic stem cells and HIV infection. *J*
426 *Infect Dis* **207**, 1790-1792, doi:10.1093/infdis/jit120 (2013).

427 27 Hunt, P. W. *et al.* T cell activation is associated with lower CD4+ T cell
428 gains in human immunodeficiency virus-infected patients with sustained viral
429 suppression during antiretroviral therapy. *J Infect Dis* **187**, 1534-1543,
430 doi:10.1086/374786 (2003).
431 28 Isgro, A. *et al.* Altered clonogenic capability and stromal cell function
432 characterize bone marrow of HIV-infected subjects with low CD4+ T cell counts
433 despite viral suppression during HAART. *Clin Infect Dis* **46**, 1902-1910,
434 doi:10.1086/588480 (2008).
435 29 Shirozu, M. *et al.* Structure and chromosomal localization of the human
436 stromal cell-derived factor 1 (SDF1) gene. *Genomics* **28**, 495-500,
437 doi:10.1006/geno.1995.1180 (1995).
438 30 Moll, N. M. & Ransohoff, R. M. CXCL12 and CXCR4 in bone marrow
439 physiology. *Expert Rev Hematol* **3**, 315-322, doi:10.1586/ehm.10.16 (2010).
440 31 Petrie, H. T. Cell migration and the control of post-natal T-cell
441 lymphopoiesis in the thymus. *Nat Rev Immunol* **3**, 859-866, doi:10.1038/nri1223
442 (2003).
443 32 Nixon, C. C. *et al.* HIV-1 infection of hematopoietic progenitor cells in vivo
444 in humanized mice. *Blood* **122**, 2195-2204, doi:10.1182/blood-2013-04-496950
445 (2013).
446 33 Carter, C. C. *et al.* HIV-1 utilizes the CXCR4 chemokine receptor to infect
447 multipotent hematopoietic stem and progenitor cells. *Cell Host Microbe* **9**, 223-234,
448 doi:10.1016/j.chom.2011.02.005 (2011).
449 34 Ho Tsong Fang, R., Colantonio, A. D. & Uittenbogaart, C. H. The role of
450 the thymus in HIV infection: a 10 year perspective. *AIDS* **22**, 171-184,
451 doi:10.1097/QAD.0b013e3282f2589b (2008).

452 35 Bordoni, V. *et al.* Early ART in primary HIV infection may also preserve
453 lymphopoiesis capability in circulating haematopoietic progenitor cells: a case report.
454 *J Antimicrob Chemother*, doi:10.1093/jac/dku559 (2015).
455 36 Akkina, R. New insights into HIV impact on hematopoiesis. *Blood* **122**,
456 2144-2146, doi:10.1182/blood-2013-08-518274 (2013).
457 37 Dorival, C. *et al.* HIV-1 Nef protein expression in human CD34+
458 progenitors impairs the differentiation of an early T/NK cell precursor. *Virology* **377**,
459 207-215, doi:10.1016/j.virol.2008.04.009 (2008).
460 38 Hoebeke, I. *et al.* T-, B- and NK-lymphoid, but not myeloid cells arise from
461 human CD34(+)CD38(-)CD7(+) common lymphoid progenitors expressing
462 lymphoid-specific genes. *Leukemia* **21**, 311-319, doi:10.1038/sj.leu.2404488 (2007).
463 39 Awong, G. *et al.* Characterization in vitro and engraftment potential in vivo
464 of human progenitor T cells generated from hematopoietic stem cells. *Blood* **114**,
465 972-982, doi:10.1182/blood-2008-10-187013 (2009).
466 40 Bordoni, V. *et al.* Bone Marrow CD34+ Progenitor Cells from HIV-
467 Infected Patients Show an Impaired T Cell Differentiation Potential Related to
468 Proinflammatory Cytokines. *AIDS Res Hum Retroviruses* **33**, 590-596,
469 doi:10.1089/aid.2016.0195 (2017).
470 41 Savkovic, B. *et al.* A quantitative comparison of anti-HIV gene therapy
471 delivered to hematopoietic stem cells versus CD4+ T cells. *PLoS Comput Biol* **10**,
472 e1003681, doi:10.1371/journal.pcbi.1003681 (2014).
473 42 Liu, Y., Zhou, J., Pan, J. A., Mabiala, P. & Guo, D. A novel approach to
474 block HIV-1 coreceptor CXCR4 in non-toxic manner. *Mol Biotechnol* **56**, 890-902,
475 doi:10.1007/s12033-014-9768-7 (2014).

476 43 Suzuki, K., Ahlenstiel, C., Marks, K. & Kelleher, A. D. Promoter Targeting
477 RNAs: Unexpected Contributors to the Control of HIV-1 Transcription. *Mol Ther*
478 *Nucleic Acids* **4**, e222, doi:10.1038/mtna.2014.67 (2015).
479 44 Costin, J. M. Cytopathic mechanisms of HIV-1. *Virol J* **4**, 100,
480 doi:10.1186/1743-422x-4-100 (2007).
481 45 Tsukamoto, T., Yamamoto, H., Okada, S. & Matano, T. Recursion-based
482 depletion of human immunodeficiency virus-specific naive CD4(+) T cells may
483 facilitate persistent viral replication and chronic viraemia leading to acquired
484 immunodeficiency syndrome. *Med Hypotheses* **94**, 81-85,
485 doi:10.1016/j.mehy.2016.06.024 (2016).
486 46 Su, L. *et al.* HIV-1-induced thymocyte depletion is associated with indirect
487 cytopathogenicity and infection of progenitor cells in vivo. *Immunity* **2**, 25-36
488 (1995).
489 47 Adachi, A. *et al.* Production of acquired immunodeficiency syndrome-
490 associated retrovirus in human and nonhuman cells transfected with an infectious
491 molecular clone. *J Virol* **59**, 284-291 (1986).
492 48 Holmes, R. & Zuniga-Pflucker, J. C. The OP9-DL1 system: generation of
493 T-lymphocytes from embryonic or hematopoietic stem cells in vitro. *Cold Spring*
494 *Harb Protoc* **2009**, pdb.prot5156, doi:10.1101/pdb.prot5156 (2009).
495 49 Tsukamoto, T. & Okada, S. The use of RetroNectin in studies requiring in
496 vitro HIV-1 infection of human hematopoietic stem/progenitor cells. *J Virol*
497 *Methods* **248**, 234-237, doi:10.1016/j.jviromet.2017.08.003 (2017).
498 50 Suzuki, K. *et al.* Prolonged transcriptional silencing and CpG methylation
499 induced by siRNAs targeted to the HIV-1 promoter region. *J RNAi Gene Silencing* **1**,
500 66-78 (2005).

Acknowledgements

This work was supported by the National Health and Medical Research Council, Australia (project grant). It was also partially supported by grants from the following organizations: the Japan Agency for Medical Research and Development (Research program on HIV/AIDS, No. 16fk0410108h0001); Ministry of Education, Culture, Sports, Science and Technology, Japan (Grants-in-Aid for Science Research, No. 25114711) and Kumamoto University (AIDS International Collaborative Research Grant). I thank Drs. Kazuo Matsui and Shoichi Kawakami of Fukuda Hospital, Kumamoto, Japan for their assistance with cord blood sampling. I thank Prof. Seiji Okada of Center for AIDS Research, Kumamoto University and his staff for their assistance with preparing resources. I thank Prof. Anthony D Kelleher and Dr. Kazuo Suzuki of the Kirby Institute for infection and immunity in society, UNSW Australia for their support. I thank Enago (www.enago.jp) for the English language review.

Author information

The author declares no competing financial interests associated with the present work. Correspondence and requests for materials should be addressed to ttsukamoto@med.kindai.ac.jp.

520 **Figures**

521

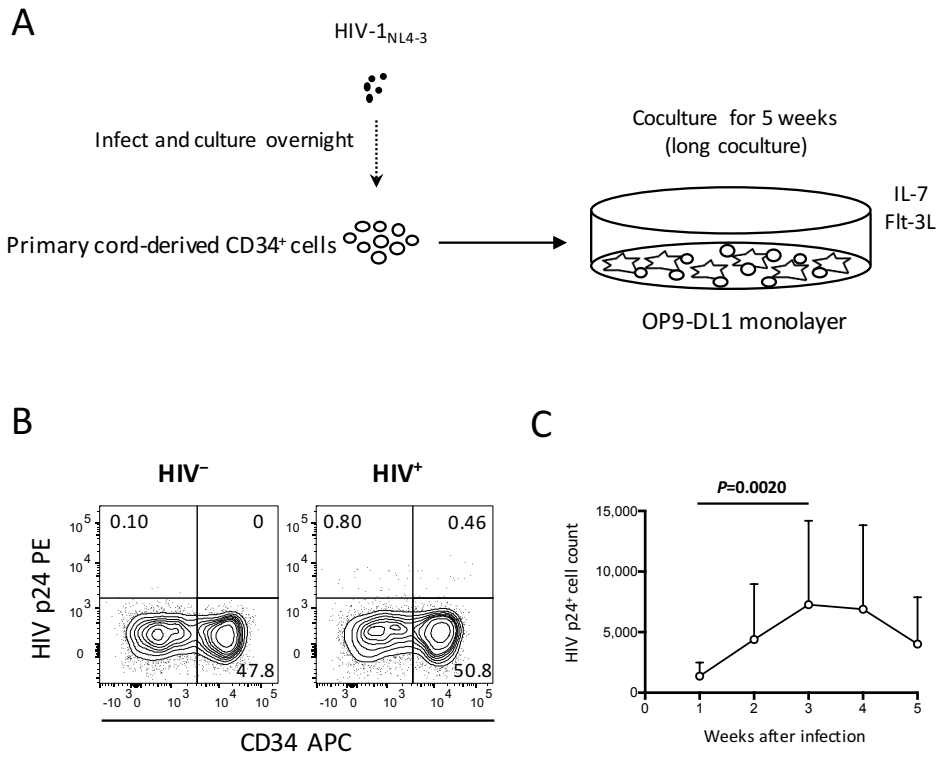

522

523 **Figure 1.** Primary umbilical cord-derived CD34$^+$ cells are susceptible to HIV
524 infection. Coculture of HIV-infected primary cord-derived CD34$^+$ cells with OP9-
525 DL1 cells resulted in persistent viral replication for 5 weeks (n = 12). (A) Schematic
526 representation of experiment 1 (long coculture). Cord-derived CD34$^+$ cells were
527 infected with HIV-1$_{NL4-3}$ and cocultured with OP9-DL1 cells for 5 weeks. (B)
528 Intracellular HIV p24 expression was tested 1 week after infection. HIV p24$^+$ cells
529 were found in both the CD34$^+$ and CD34$^-$ fractions of HIV-infected samples.
530 Representative plots are shown. (C) HIV p24$^+$ cell counts at weeks 1–5 post-infection
531 (n = 12). Statistical analyses were performed using the Wilcoxon matched-pairs
532 signed rank test.

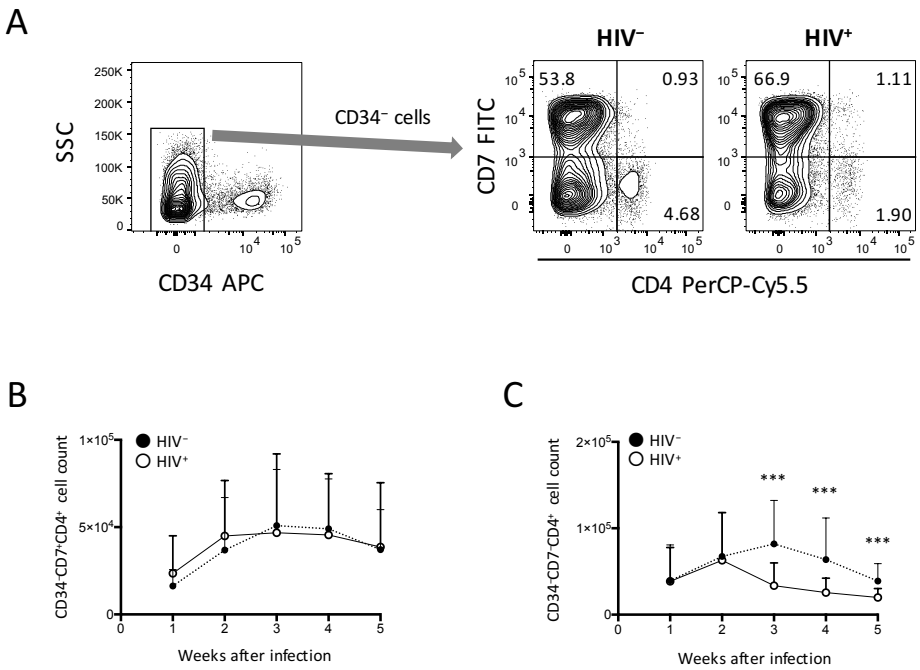

533

534 **Figure 2.** Pre-exposure of primary cord-derived CD34$^+$ cells to HIV-1 affected the
535 dynamics of OP9-DL1 cocultured cells (n = 12). (A) Representative plots showing the
536 loss of CD34$^-$CD7$^-$CD4$^+$ cells in the HIV-infected cocultures 3–5 weeks after
537 infection. (B-C) Cell counts were compared between HIV$^+$ and HIV$^-$ cocultures for
538 (B) CD34$^-$CD7$^+$CD4$^+$ and (C) CD34$^-$CD7$^-$CD4$^+$ cells. Statistical analyses were
539 performed using the Wilcoxon matched-pairs signed rank test. ***: $P < 0.001$.

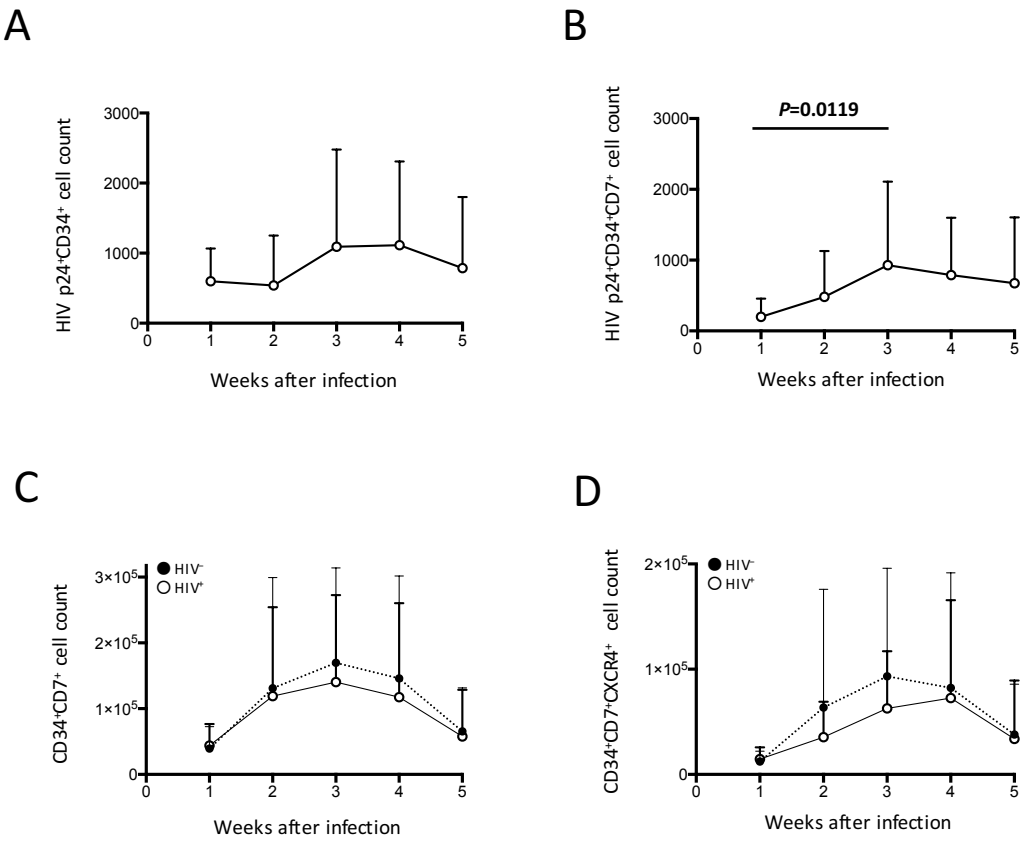

Figure 3. Pre-exposure of primary cord-derived $CD34^+$ cells to HIV-1 affected the dynamics of $CD34^+$ cells in the subsequent OP9-DL1 cocultures (n = 12). (A) HIV $p24^+CD34^+$ cell counts in HIV^+ OP9-DL1 cocultures. (B) HIV $p24^+CD34^+CD7^+$ cell counts in HIV^+ OP9-DL1 cocultures. (C–D) Cell counts were compared between HIV^+ and HIV^- cocultures for (C) $CD34^+CD7^+$ and (D) $CD34^+CD7^+CXCR4^+$ cells. Statistical analyses were performed using the Wilcoxon matched-pairs signed rank test.

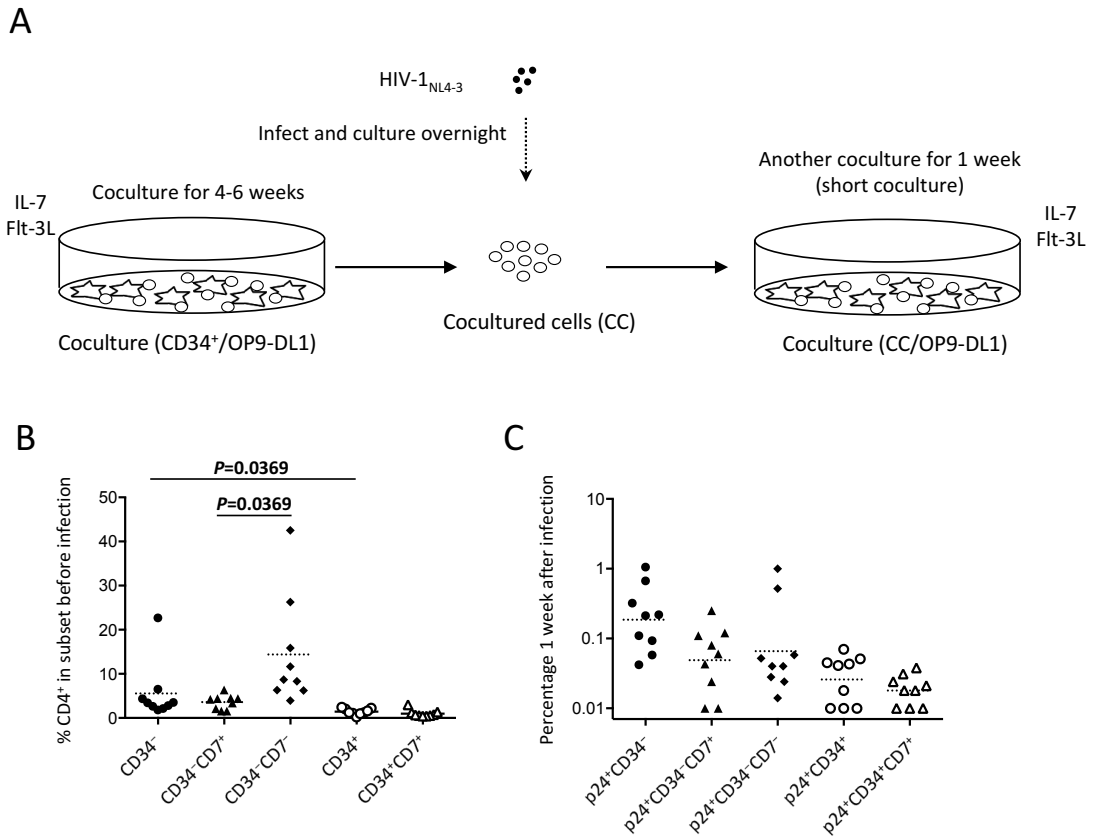

Figure 4. Experiment 2 (short coculture, n = 9) was performed to further analyse the dynamics of $CD34^+$ cells in the presence of HIV-1. (A) Schematic representation of experiment 2 (short coculture). Primary cord-derived $CD34^+$ cells were cocultured with OP9-DL1 cells for 4–6 weeks. Cells were then collected and infected with HIV-1_{NL4-3}. The infected cells were cocultured again with OP9-DL1 cells for 1 week, collected and analysed. (B) Percentages of $CD4^+$ cells in $CD34^-$, $CD34^-CD7^+$, $CD34^-CD7^-$, $CD34^+$ and $CD34^+CD7^+$ subsets before infection. A multiple comparison test was performed to compare $CD34^-$ and $CD34^+$ cells or $CD34^-CD7^+$ and $CD34^-CD7^-$ cells. (C) Frequencies of HIV $p24^+$, $p24^+CD34^-CD7^+$, $p24^+CD34^-CD7^-$, $p24^+CD34^+$ and $p24^+CD34^+CD7^+$ cells measured 1 week after the second post-infection coculture (n = 9). Statistical analysis was performed using the multiple comparison test with Dunn's method.

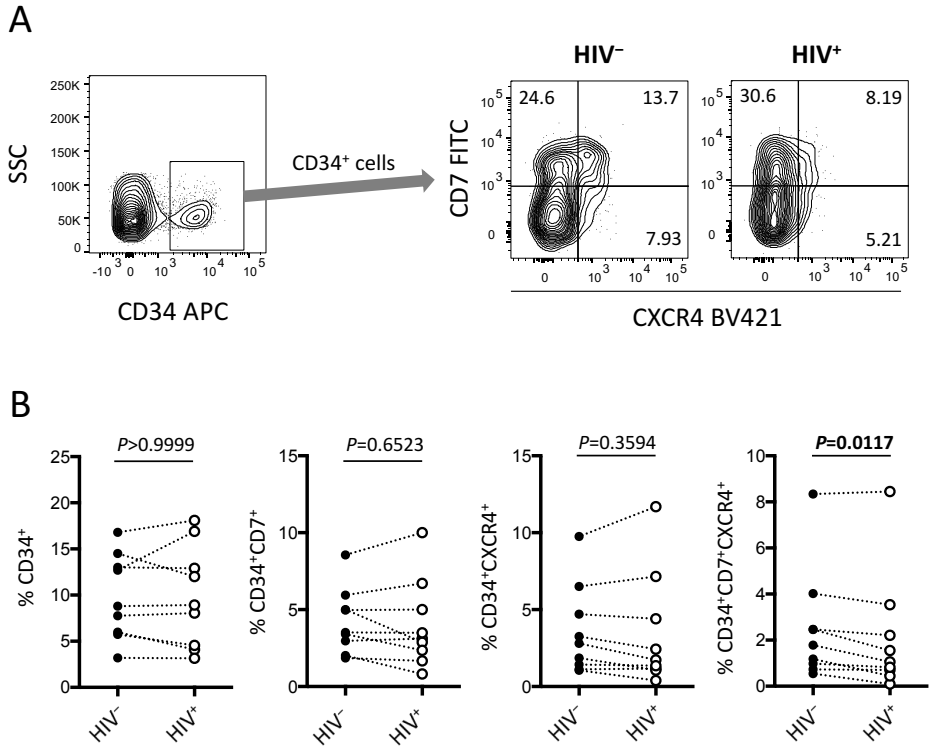

Figure 5. CD34$^+$ cells in experiment 2 (short coculture, n = 9) were analysed 1 week after the second post-infection coculture. (A) Representative plots showing CD7/CXCR4 expression levels in CD34$^+$ cells. An HIV$^+$ sample is compared to its autologous uninfected counterpart. (B) Frequencies of CD34$^+$ (left), CD34$^+$CD7$^+$ (middle left), CD34$^+$CXCR4$^+$ (middle right) and CD34$^+$CD7$^+$CXCR4$^+$ (right) cells were compared between HIV$^+$ and HIV$^-$ samples. Statistical analyses were performed using the Wilcoxon matched-pairs signed rank test.

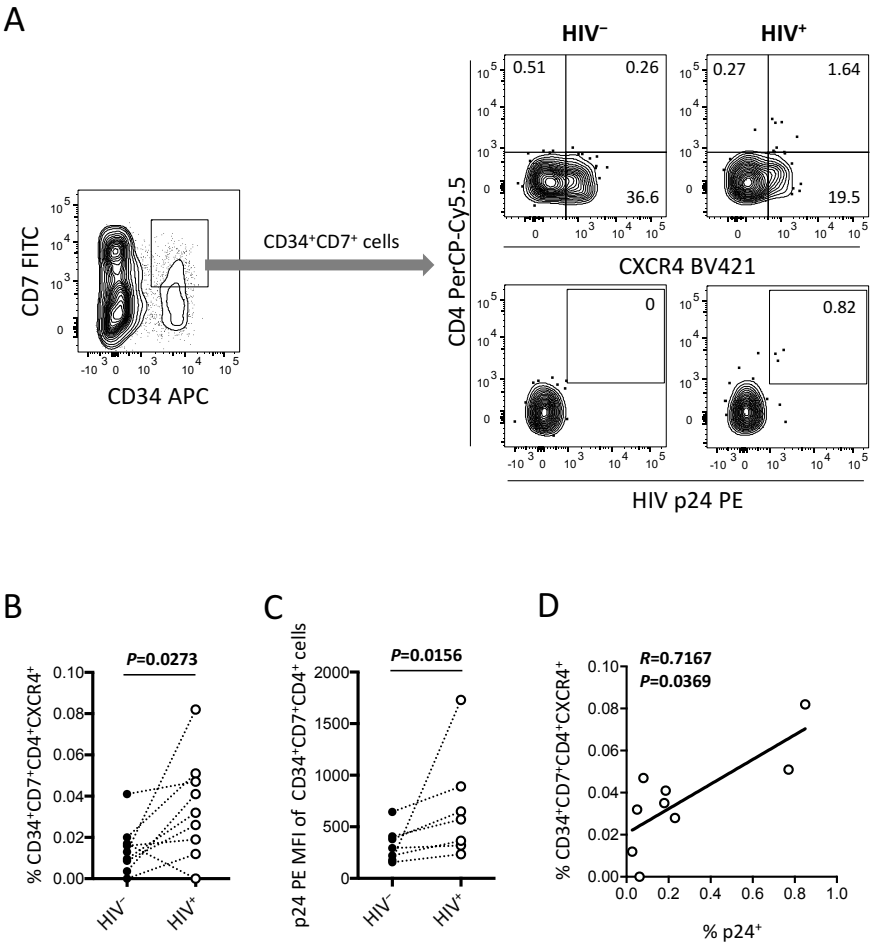

Figure 6. $CD34^+CD7^+$ cells in experiment 2 (short coculture, n = 9) were analysed 1 week after the second post-infection coculture. For these analyses, compensation matrices were checked carefully to exclude false-positive events. (A) Representative plots showing CD4/CXCR4 and CD4/p24 expression levels in $CD34^+CD7^+$ cells. An HIV^+ sample is compared to its autologous uninfected counterpart. (B) Comparison of the frequencies of $CD34^+CD7^+CD4^+CXCR4^+$ cells between HIV^+ and HIV^- samples. (C) p24 mean fluorescence intensities (MFIs) of $CD34^+CD7^+CD4^+$ cells were compared between HIV^+ and HIV^- samples (n = 7). (D) The frequencies of $CD34^+CD7^+CD4^+CXCR4^+$ cells were correlated with those of $p24^+$ cells. Comparisons were performed using the Wilcoxon matched-pairs signed rank test. Spearman's correlation coefficient was calculated for the correlation analysis.

581 **Extended Data figures and tables**
582

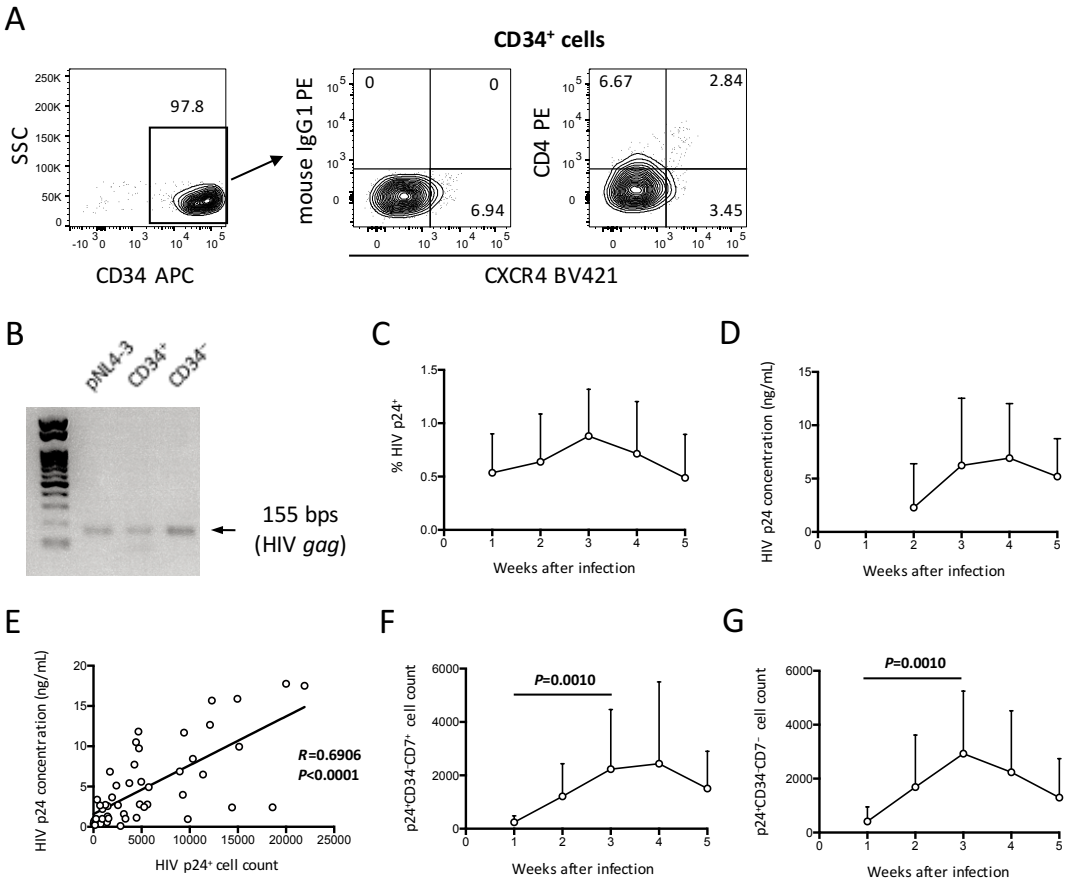

583
584 **Extended Data Figure 1.** HIV infection of cord-derived CD34$^+$ cells and derivatives
585 were evaluated. (A) Primary cord-derived CD34$^+$ cells were gated and tested for CD4
586 and CXCR4 expression by flow cytometry. Representative plots are shown. The CD4
587 signal levels were compared to the signal levels of a PE-conjugated mouse isotype
588 control antibody. (B) The CD34$^+$ and CD34$^-$ fractions of an HIV-infected sample
589 were separated using the CD34 microbead method. Total DNA was isolated and
590 analysed by PCR. HIV gag DNA was detected in both the CD34$^+$ and CD34$^-$
591 fractions. A PCR sample using the HIV molecular plasmid pNL4-3 was used as a
592 control. (C) Percentage of HIV p24$^+$ cells in HIV$^+$ OP9-DL1 coculture samples tested
593 weekly by intracellular staining and flow cytometry. (D) Coculture supernatants of
594 HIV-infected samples were tested for HIV p24 concentrations by ELISA at weeks 2–
595 5. (E) Correlation analysis between the frequencies of HIV p24$^+$ cells and HIV p24
596 concentrations. The weeks 2–5 data in F and G are included (n = 48). Spearman's
597 correlation coefficients are shown. (F) p24$^+$CD34$^-$CD7$^+$ cell counts. (G)
598 p24$^+$CD34$^-$CD7$^-$ cell counts. Comparisons were performed using the Wilcoxon
599 matched-pairs signed rank test.
600

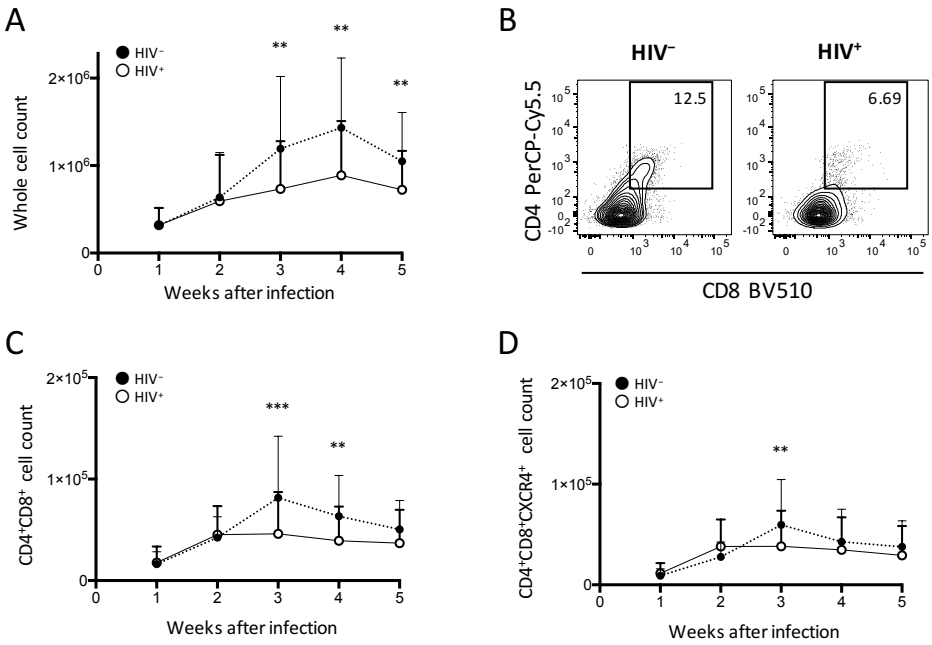

601

602 **Extended Data Figure 2.** Pre-exposure of primary cord-derived $CD34^+$ cells to HIV-
603 1 affected the dynamics of OP9-DL1 cocultured cells. (A) Whole cell counts were
604 compared between HIV^+ and HIV^- cocultures. (B) Representative plots for samples
605 displaying reduced frequencies of $CD4^+CD8^+$ cells 3–5 weeks after HIV pre-exposure
606 of primary $CD34^+$ cells and coculture. The plots were selected from week 4 samples.
607 (C–D) Cell counts were compared between HIV^+ and HIV^- cocultures for (C)
608 $CD4^+CD8^+$ and (D) $CD4^+CD8^+CXCR4^+$ cells. Statistical analyses were performed
609 using the Wilcoxon matched-pairs signed rank test. **: $P < 0.01$, ***: $P < 0.001$.

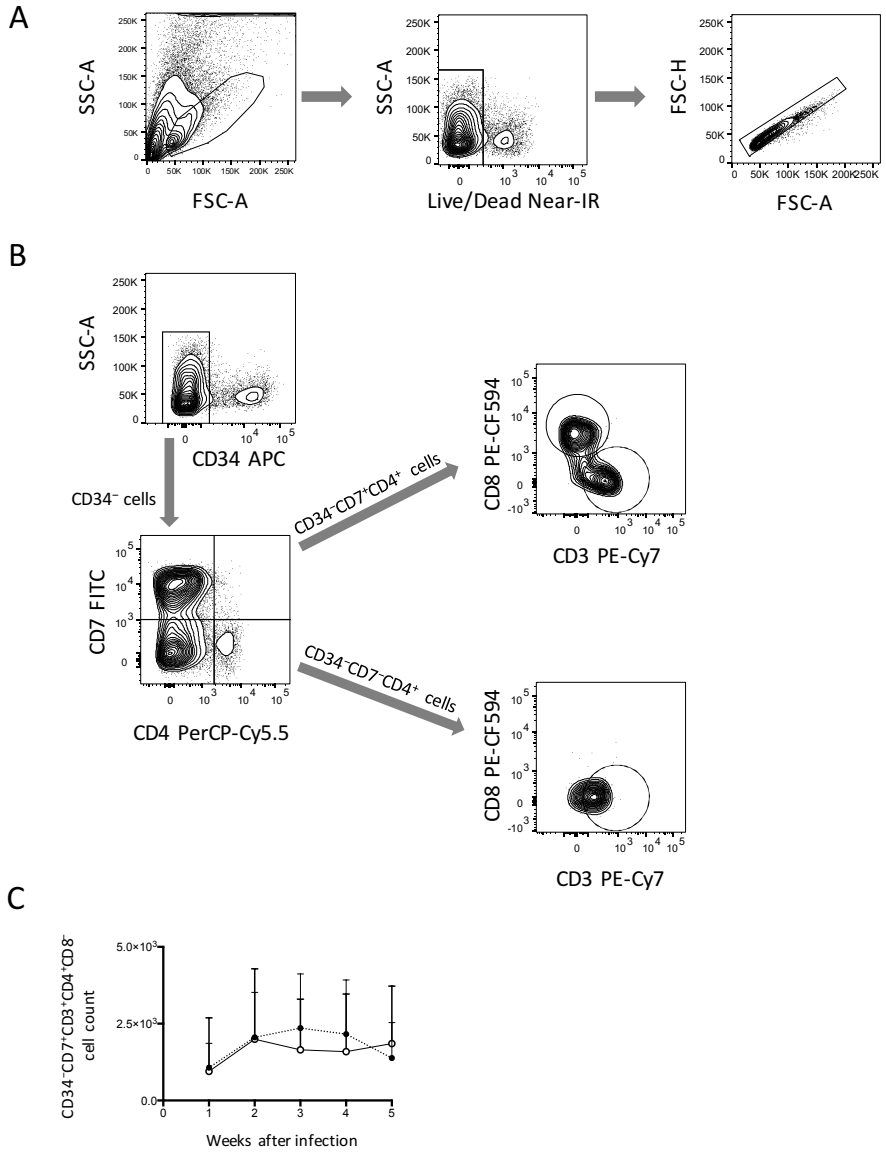

610

611 **Extended Data Figure 3.** Gating strategies and analysis of $CD34^{-}CD4^{+}$ cells. (A)
612 Flow cytometry plots showing the gates for lymphoid cells (left), live cells (middle),
613 and singlet cells (right). (B) Flow cytometry plots showing the phenotype analysis of
614 $CD34^{-}CD4^{+}$ cells in an OP9-DL1 coculture. Representative plots are shown. Cord-
615 derived $CD34^{+}$ cells were cocultured with OP9-DL1 cells for 4 weeks. Cells were
616 collected and analysed by flow cytometry. $CD34^{-}$ cells were gated by CD7 and CD4
617 expression. $CD7^{+}CD4^{+}$ and $CD7^{-}CD4^{+}$ cells were further gated by CD8 and CD3
618 expression. The analysis revealed that $CD7^{+}CD4^{+}$ cells contained different subsets
619 including $CD3^{-}CD4^{+}CD8^{+}$ and $CD3^{+}CD4^{+}CD8^{-}$ cells, whereas $CD7^{-}CD4^{+}$ cells were
620 mostly $CD3^{+}CD4^{+}CD8^{-}$ cells. These results indicate that CD4/CD8 double-positive
621 thymocytes, $CD7^{+}$ CD4 T cells and $CD7^{-}$ CD4 T cells were generated via coculture of
622 cord-derived $CD34^{+}$ and OP9-DL1 cells. (C) $CD34^{-}CD7^{+}CD3^{+}CD4^{+}CD8^{-}$ cell counts.

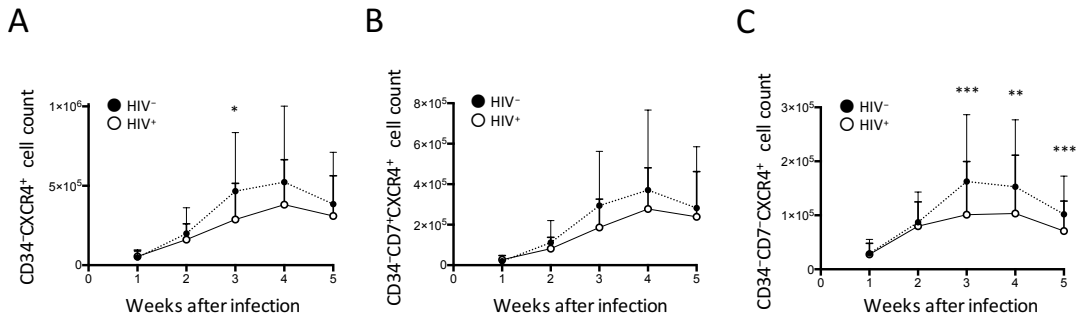

Extended Data Figure 4. Phenotypes of $CD34^{-}$ cells in the OP9-DL1 cocultures were analysed weekly for 5 weeks after HIV-1 infection. Cell counts were compared with those in uninfected samples. (A) $CD34^{-}CXCR4^{+}$ cell counts. (B) $CD34^{-}CD7^{+}CXCR4^{+}$ cell counts. (C) $CD34^{-}CD7^{-}CXCR4^{+}$ cell counts. Comparisons were performed using the Wilcoxon matched-pairs signed rank test. *: $P < 0.05$, **: $P < 0.01$, ***: $P < 0.001$.

630

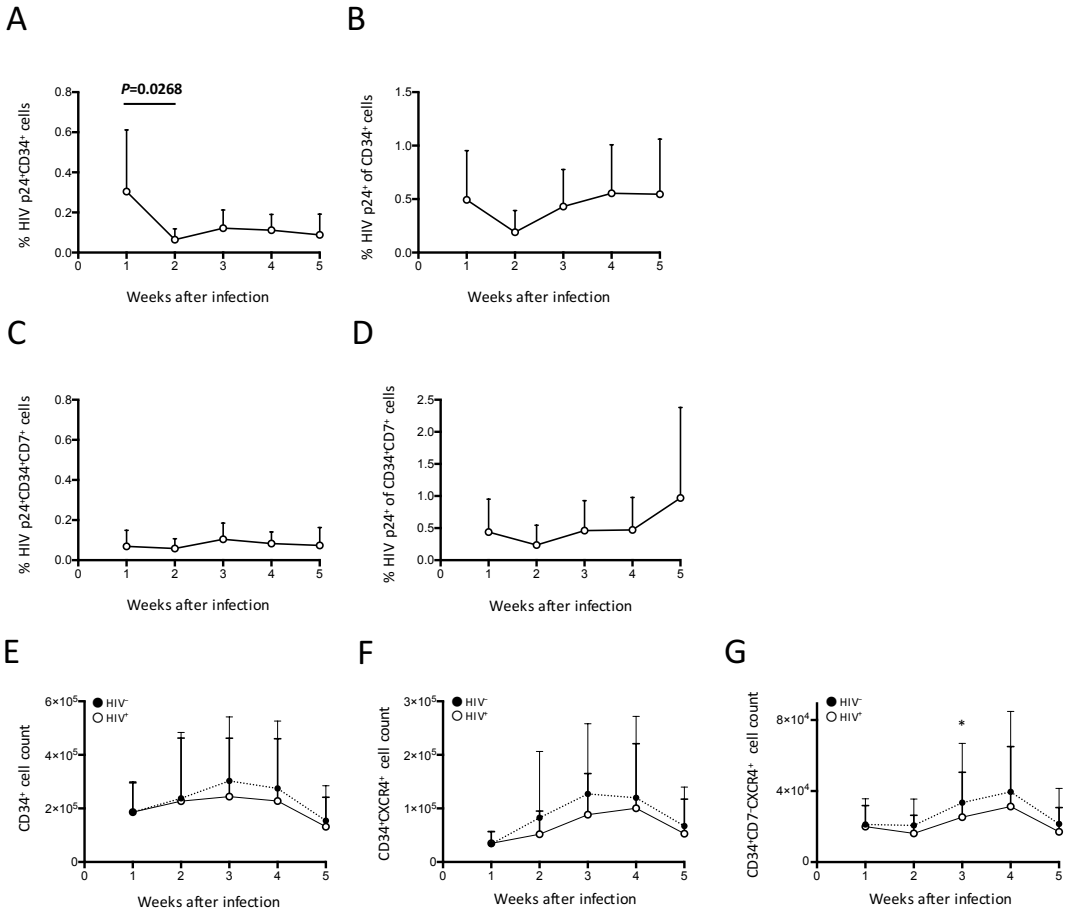

631

632 **Extended Data Figure 5.** (A–D) HIV p24^{+} subset dynamics were analysed. (A)
633 Percent p24^{+}CD34^{+} cells. (B) Percent p24^{+} cells among CD34^{+} cells. (C) Percent
634 p24^{+}CD34^{+}CD7^{+} cells. (D) Percent p24^{+} cells among CD34^{+}CD7^{+} cells. (E–G)
635 CD34^{+} subset dynamics were analysed and compared between HIV^{+} and HIV^{-}
636 samples. (E) CD34^{+} cell counts. (F) CD34^{+}CXCR4^{+} cell counts. (G)
637 CD34^{+}CD7^{-}CXCR4^{+} cell counts.

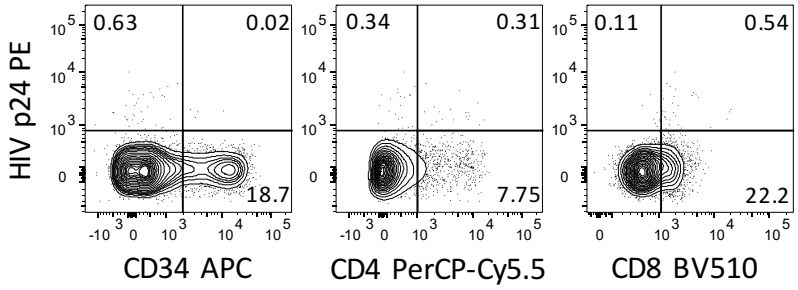

638

639 **Extended Data Figure 6.** Experiment 2 (short coculture, n = 9) was performed to
640 further analyse the dynamics of $CD34^+$ cells in the presence of HIV-1. Representative
641 plots showing HIV $p24^+$ cells 1 week after infection. The majority of $p24^+$ cells were
642 $CD34^-$ (left). HIV replication may be causing CD4 downregulation (middle).
643 Frequencies of $CD8^+$ cells in $p24^+$ cells were variable among the samples (right).

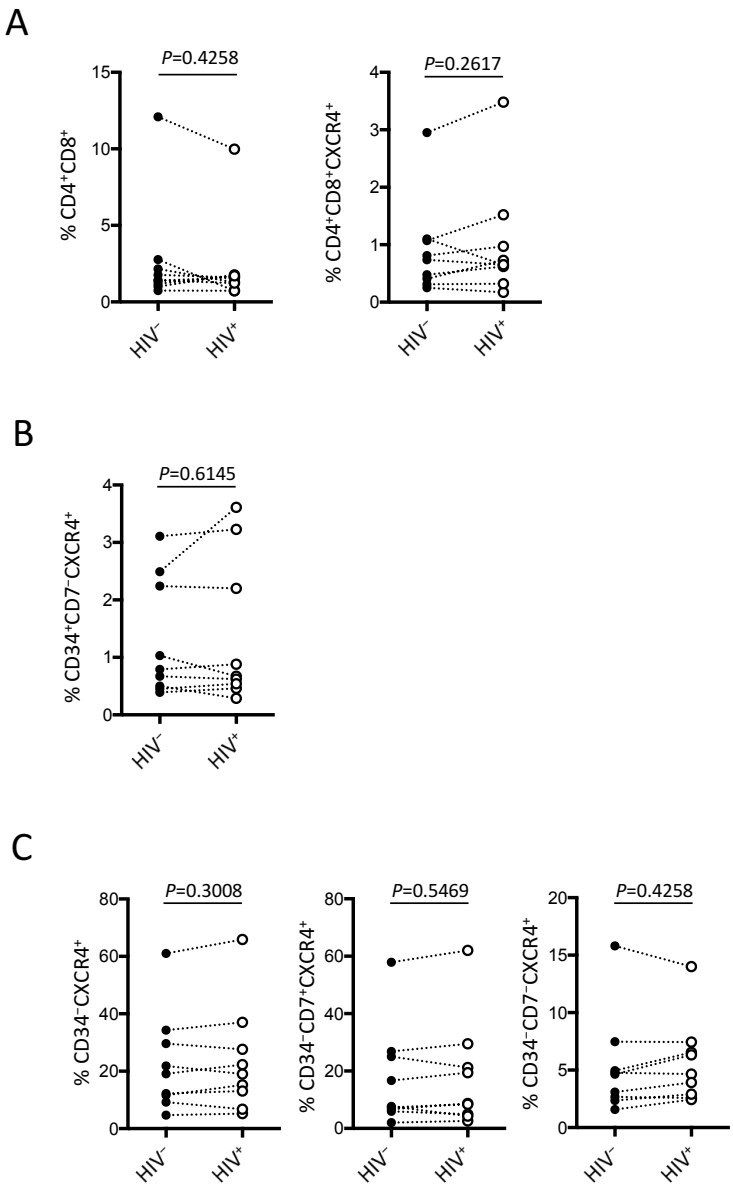

644

645 **Extended Data Figure 7.** The frequencies of subsets were compared between HIV-
646 infected and uninfected samples 1 week after infection. (A) $CD4^{+}CD8^{+}$ cells. (B)
647 $CD4^{+}CD8^{+}CXCR4^{+}$ cells. (C) $CD34^{-}CXCR4^{+}$ (left), $CD34^{-}CD7^{+}CXCR4^{+}$ (middle)
648 and $CD34^{-}CD7^{-}CXCR4^{+}$ (right) cells. Comparisons were performed using the
649 Wilcoxon matched-pairs signed rank test.

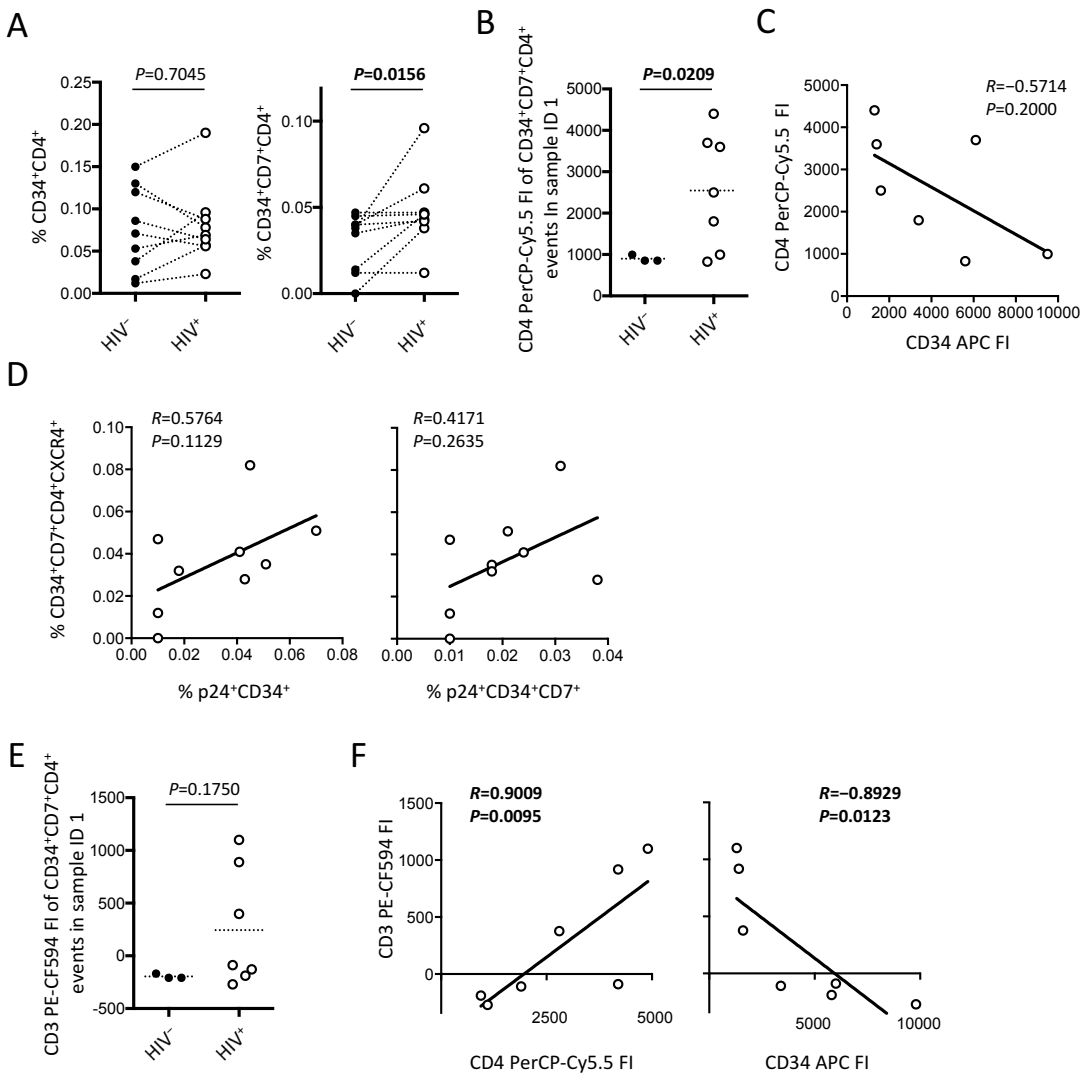

Extended Data Figure 8. $CD34^+CD7^+CD4^+$ cells were further analysed. (A) Comparison of $CD34^+CD4^+$ (left) and $CD34^+CD7^+CD4^+$ (right) frequencies between HIV^+ and HIV^- samples. (B) Fluorescence intensities (FIs) of $CD34^+CD7^+CD4^+$ cells were compared between HIV^+ and HIV-$^-$ samples using the Mann-Whitney test. (C) Correlation between the CD4 and CD34 FI of $CD34^+CD7^+CD4^+$ cells in the HIV^+ sample of ID 1 were analysed (n = 3 for HIV^-; n = 7 for HIV^+). (D) $CD34^+CD7^+CD4^+CXCR4^+$ cells were tested for correlations with the frequencies of $p24^+CD34^+$ (left) and $p24^+CD34^+CD7^+$ (right) cells. (E) Comparison of CD3 FIs between HIV-infected and uninfected samples. (F) Correlation analysis between CD3 FIs and CD4 (left) or CD34 (right) FIs. Comparisons were made using the Wilcoxon matched-pairs signed rank test unless otherwise noted. Spearman's correlation coefficients were calculated for correlation analyses.

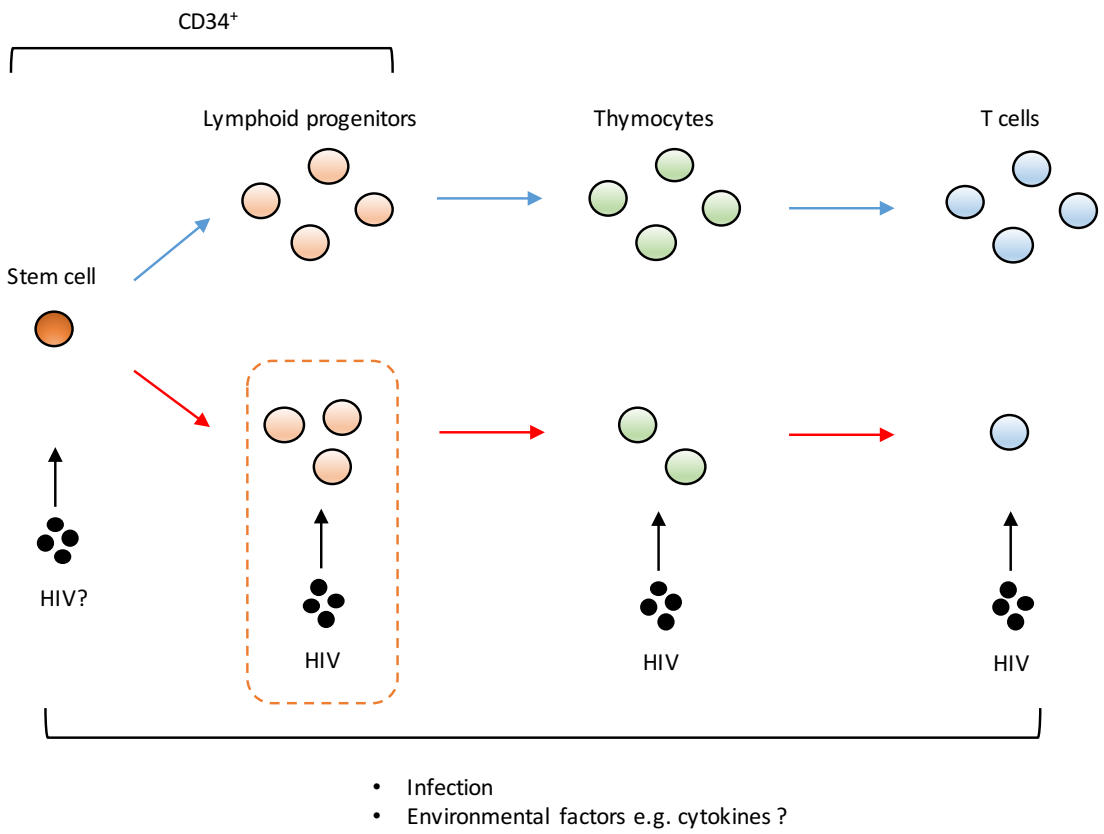

Extended Data Figure 9. A schematic representation of factors potentially influencing the decrement of $CD4^+$ T cells. Thymocytes and T cells are highly susceptible to HIV infection. However, the decrease of $CD34^+$ lymphoid progenitor counts occurs early and precedes the decrease of thymocyte and T-cell counts. Although the mechanisms for the decrease of $CD34^+$ lymphoid progenitors are unclear, this decline may limit the production of thymocytes and T cells.

670

Subset	Cell count in infected samples (mean ± SD, n = 4)	Percentage in the mean whole-cell count
Whole	390,000 ± 155,000	100
$p24^+$	547 ± 258	0.140
$p24^+CD34^-CD7^+$	326 ± 242	0.084
$p24^+CD34^-CD7^-$	124 ± 56	0.032
$p24^+CD34^+$	97 ± 42	0.025
$p24^+CD34^+CD7^+$	80 ± 31	0.021

671

672 **Extended Data Table 1.** Mean cell counts (n = 4) in different HIV $p24^+$ subsets of
673 OP9-DL1 cocultured cells. The whole-cell count data were obtained using four of
674 nine samples from experiment 2 (short coculture), in which cord-derived $CD34^+$ cells
675 were first cocultured with OP9-DL1 cells for 4–6 weeks, infected with HIV-1_{NL4-3},
676 cocultured again for 1 week and analyzed by flow cytometry. The percentages in the
677 mean whole-cell count are also shown, and they are comparable to those presented in
678 Fig. 4C. SD, standard deviation.

679

Subset	Cell count (mean ± SD, n = 4)		$\% \frac{(Infected - Uninfected)}{Uninfected}$
	Uninfected	*Infected*	
Whole	400,000 ± 169,000	390,000 ± 155,000	−2.5
$CD4^+CD8^+$	5,790 ± 3,510	4,920 ± 2,360	**−15.0**
$CD4^+CD8^+CXCR4^+$	3,290 ± 1,760	3,050 ± 1,840	−7.3
$CD34^+$	32,800 ± 18,200	32,100 ± 21,400	−2.3
$CD34^+CD7^+$	16,700 ± 9,500	16,100 ± 12,100	−3.6
$CD34^+CXCR4^+$	18,300 ± 11,000	18,300 ± 14,700	−0.1
$CD34^+CD7^+CXCR4^+$	12,100 ± 7,800	11,900 ± 11,100	−2.0
$CD34^+CD7^-CXCR4^+$	6,150 ± 3,870	6,380 ± 3,990	+3.7
$CD34^+CD7^+CD4^+$	129 ± 42	178 ± 74	**+38.0**
$CD34^-CXCR4^+$	148,000 ± 164,000	157,000 ± 167,000	+5.8
$CD34^-CD7^+CXCR4^+$	131,000 ± 161,000	139,000 ± 162,000	+5.6
$CD34^-CD7^-CXCR4^+$	16,900 ± 7,500	18,300 ± 8,000	+7.8

680

681 **Extended Data Table 2.** Mean cell counts (n = 4) in different subsets of OP9-DL1–
682 cocultured cells. The whole-cell count data were obtained using four of nine samples
683 from experiment 2 (short coculture), in which cord-derived $CD34^+$ cells were first
684 cocultured with OP9-DL1 for 4–6 weeks, infected with HIV-1_{NL4-3}, cocultured again
685 for 1 week and analyzed by flow cytometry. Cell counts in HIV-infected samples
686 were compared with those in uninfected control samples. Percent changes in the
687 subset cell counts following HIV infection were calculated, as shown in the right
688 column. Percent changes of >10% are shown in bold. SD, standard deviation.